

SINGLE-SHOT RESOLUTION OF X-RAY MONITOR USING CODED APERTURE IMAGING

J.W. Flanagan, M. Arinaga, H. Fukuma, H. Ikeda, T. Mitsuhashi, KEK, Tsukuba, Ibaraki, Japan
 J.S. Alexander, M.A. Palmer, D.P. Peterson, N. Rider, Cornell University, Ithaca, NY, U.S.A.
 G. Varner, University of Hawaii, Honolulu, HI, U.S.A.

Abstract

We report on tests of an x-ray beam size monitor based on coded aperture imaging [1]. This technique uses a mask pattern to modulate incoming photons, with the resulting image being deconvolved through the mask and detector responses, including the effects of diffraction and attenuation materials in the path, over the spectral and angular distribution of the synchrotron radiation generated by the beam. We have tested mask patterns called URA masks[2], which have relatively flat spatial frequency response, and an open aperture of 50% for high-flux throughput, enabling single-shot (bunch-by-bunch, turn-by-turn) measurements without the need for heat-sensitive mirrors. Bunch size measurements of ~10 micron bunches with single-shot (statistics-dominated) resolutions of ~2.5 microns have been demonstrated at CEsrTA, and single-shot measurements with similar or better resolution of beams in the ~5 micron range are being aimed for at the ATF2. A beam-size monitor based on these principles is also being designed for the SuperKEKB low-emittance rings. We present estimated single-shot resolutions, along with a comparison to single-shot resolution measurements made at CEsrTA.

INTRODUCTION

We are developing beam size diagnostics based on coded aperture imaging for low-emittance beams, such as the SuperKEKB Low Emittance Ring (LER) and High Emittance Ring (HER), CEsrTA and the ATF2; Table 1 shows x-ray source parameters for each machine. For this purpose, we use x-ray monitors based on coded aperture imaging. For the mask pattern, we use URA masks, which feature resolutions on the order of, or a bit better than, simple pinholes, with a wide aperture, broad-band (non-monochromatic) response and relatively flat spatial frequency response for wide dynamic range in beam sizes.

Table 1: X-ray Source Parameters

Parameter	CesrTA (low-energy)	ATF2	SuperKEKB LER / HER
ϵ_y (pm-rad) (min)	<20	~30	~10
σ_y (μm) (min.)	~10	~4	~10
Beam Energy (GeV)	2.085	1.3	4 / 7
Bending radius (m)	31.65	4.3	31.74 / 106
Critical Energy (keV)	0.63	1.1	4.4 / 7.1

As has been described previously[3], the expected image at the detector plane from a point source is calculated from the σ and π components of the complex wavefront amplitude $A_{\sigma,\pi}$ of the component of synchrotron radiation (SR) for each wavelength in the source spectrum[4]. Each component is propagated through a model of the beamline, taking account of the attenuation and phase shifts due to the various materials and path lengths along the way, with a Kirchhoff integral over the surface of the mask [5]:

$$A_{\sigma,\pi}(Detector) = \frac{iA_{\sigma,\pi}(Source)}{\lambda} \times \int_{mask} \frac{t(y_m)}{r_1 r_2} e^{i\frac{2\pi}{\lambda}(r_1+r_2)} \left(\frac{\cos\theta_1 + \cos\theta_2}{2} \right) dy_m$$

where $t(y_m)$ is the complex transmission of the mask element at position y_m . Intensities of each wavelength and polarization component are summed at location on the detector. We consider here only vertical beam size measurement, where the detector is considered to be a vertical linear array of pixels.

The source beam is considered to be a vertical distribution of point sources. The above formulation can also be applied to sources with non-zero angular dispersion and longitudinal extent, for a more accurate simulation of emittance and source-depth effects. However, for the machines under consideration here these effects are estimated to be negligibly small, so for computational speed we restrict ourselves to 1-dimensional vertical distributions.

ESTIMATES OF STATISTICS-LIMITED SINGLE-SHOT RESOLUTIONS

At low intensities, the resolution of the system is limited by statistical fluctuations in the number of detected photons. To estimate the resolution of the system as a function of beam size, simulated images are calculated for Gaussian beams of various sizes. The simulated detector images for different-sized beams are then compared pair-wise against each other, with one image in a pair representing a measured image for a known beam size, and the other image representing a proposed model. The differences between the two images in signal heights for each detector channel are used to evaluate the χ^2 per degree of freedom for this “fit” [6]:

$$\frac{\chi^2}{\nu} = \frac{1}{N - n - 1} \sum_{i=1}^N \frac{[s'_i - s_i]^2}{\sigma_i^2},$$

where N is the number of detector channels (pixels), n is the number of fit parameters, which in this case is one, normalization. For a 32-pixel detector, the number of degrees of freedom, ν ($N-n-1$) is then taken to be 30. The residual weighting function σ_i for channel i is taken to be proportional to the square root of the signal height in that channel, s_i :

$$\sigma_i = \sqrt{s_i}.$$

The signal height in each channel is set to the number of expected number of photons detected in that channel for a given bunch intensity. More explicitly, the average number of photons per pixel, n_p , at the detector is calculated, and the simulated image normalized so that the average signal height is equal to n_p . Finally, the value of χ^2/ν that corresponds to a confidence interval of 68% is chosen to represent the 1- σ confidence interval.

Comparison with Data at CEsrTA

At CEsrTA, x-ray optics chips have been installed in the CHESS D Line (to view positron beams) and in the CHESS C Line (for viewing electron beams).[7] The chips installed for 2.085 GeV study operation (the “low energy” chips) contain both a URA mask coded aperture (CA) and a Fresnel zone plate. The chip consists of ~ 0.5 μm thick gold masking material on a 2.5 μm silicon substrate. (Another set of chips designed for high-power operation are also installed, but are not discussed here.) The URA mask pattern is a 31-element pattern with 10 μm , as shown in Figure 1. The detector is a 32-channel InGaAs linear array with 50 μm pixel pitch, made by Fermionics.

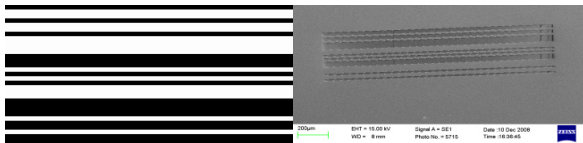


Figure 1: 31-element CA with 10 μm element size. Left: pattern. Right: SEM image from Applied Nanotools. (Adjacent elements of the same type (mask or hole) merge; there are fewer distinct regions than “elements.”)

Figure 2 shows the estimated resolution contours for the CA for an average signal height of 200 photon counts per pixel, which corresponds to 0.56 mA/bunch. Overlaid on that is the spread of measured beam sizes using the CA, taken during electron-cloud studies at CEsrTA. The bunch size varies along the bunch train due to emittance blow-up caused by the cloud, with each point representing the measured size of one bunch in the train, and the error bars representing the spread of single-turn sizes for that bunch over the course of 4096 turns. Size measurements were done by matching measured single-shot images against a range of simulated images for different sizes and positions [8]; this is similar to way the resolution plots are calculated, with the addition of a bunch offset. Figure 3 shows the measured single-shot spreads for a range of fitted beam sizes at a bunch current of 0.5 mA/bunch.

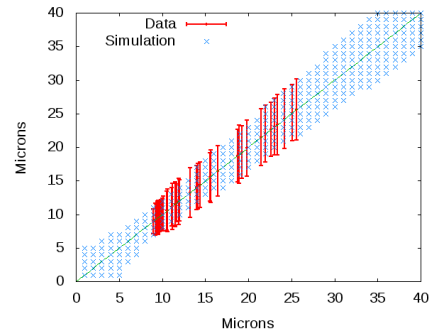


Figure 2: Calculated statistical 1- σ resolution contours for CA at CEsrTA for 200 photons/pixel (0.56 mA/bunch). Measured size spreads at 0.5 mA/bunch are overlaid.

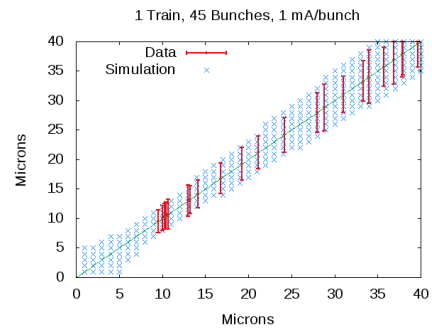


Figure 3: Calculated statistical 1- σ resolution contours for CA at CEsrTA for 200 photons/pixel (0.56 mA/bunch). Measured size spreads at 1 mA/bunch are overlaid.

The calculated statistical size spreads are between the measured spreads for 0.5 and 1.0 mA, which is expected as noise fluctuations in the detector and readout system are not included in the calculation. The shape of the estimated confidence contours and the measured spreads agree reasonably well. The measured single-shot resolution in the 10-15 μm range is ~ 2.5 μm .

Resolution Estimates at ATF2

An x-ray beam line has been constructed in the ATF2 extraction line, with the goal of testing coded aperture measurements with beam sizes down to ~ 4 -5 μm .

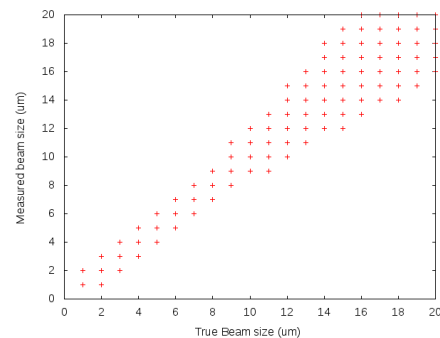


Figure 4: Calculated 1- σ statistical resolution contours for 31-element CA with 10 μm elements at the ATF2.

The minimum beam size possible at the x-ray monitor source point is expected to be below $\sim 4 \mu\text{m}$ [9]. For the ATF2, we will use a 64-channel Fermionics detector. Figure 4 shows the resolution contours for a coded aperture mask of the same type as used at CsrTA, for 1 nc bunches. As can be seen in Figure 4, statistical resolutions of $\sim 1 \mu\text{m}$ can be expected for minimum beam sizes around $4 \mu\text{m}$. Studies to measure and demonstrate this resolution are planned starting in the fall of 2011.

Resolution Estimates at SuperKEKB

The SuperKEKB Low Energy Ring (LER) and High Energy Ring (HER) will have high total beam currents, 3.6 and 2.6 A respectively, necessitating the use of a mask with much thicker substrate, such as the high-power masks being tested at CsrTA. The diagnostic beamlines will have total path lengths of around 40 m.[10] They will also have much higher critical energies than CsrTA or the ATF2, meaning that the energy of the photon spectral peak incident on the detector will be much higher. Due to the thinness of the present detector being used at CsrTA and the ATF2 ($3.5 \mu\text{m}$ InGaAs), the photon detection efficiency is low, and much of the incident flux is lost. For this reason, other types of detector are being considered, which would have higher detection efficiencies at high photon energies. For planning purposes, a set of contours assuming the use of the currently used Fermionics detector, in red, and a set of contours assuming a 10 times higher detection efficiency, in green, are calculated, assuming the use of the 59-element, $10 \mu\text{m}$ element-size CA mask pattern shown in Figure 5. The mask consists of $10 \mu\text{m}$ gold pattern on a $625 \mu\text{m}$ silicon substrate. (Other materials are also under study.)

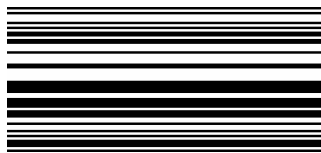


Figure 5: 59-element CA pattern for use at SuperKEKB.

Figures 6 and 7 show the expected resolution contours for the LER and HER at full bunch currents. As can be seen, with the current detector, statistical resolutions of $\sim 2 \mu\text{m}$ can be expected for beam sizes of $\sim 10 \mu\text{m}$. A future detector with improved detection efficiency would have improved statistical resolution, such that the dominant limit would be determined by detector and readout noise.

SUMMARY AND FUTURE PLANS

Estimates of the size-dependent statistical resolution of a coded aperture mask have been compared with data. The measured confidence intervals are, as expected, a bit larger than would be explained purely by photon statistics, but the spreads seem to be in reasonable agreement with the calculated resolutions as a function of beam size. The same estimation procedure has been applied to the ATF2 and SuperKEKB. The ATF2 beamline has been

constructed, and data taking is anticipated in Autumn 2011. SuperKEKB commissioning is planned in 2014.

Further topics to be pursued are absolute calibration checks at CsrTA, reconstruction methods for best recovering full profile and position information, and development of detector and read-out systems for SuperKEKB, with improved photon detection efficiency at the higher energy photons that will be generated there.

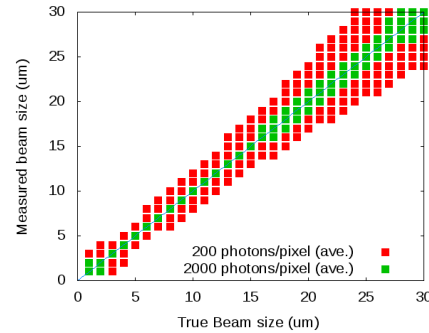


Figure 6: Calculated $1\text{-}\sigma$ statistical resolution contours for coded aperture mask at the SuperKEKB HER.

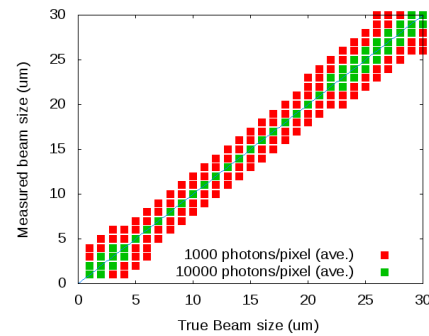


Figure 7: Calculated $1\text{-}\sigma$ statistical resolution contours for coded aperture mask at the SuperKEKB LER.

ACKNOWLEDGMENTS

We thank the Cornell CHSS group for their assistance in x-ray beam line set up at CsrTA, as well as the many students who have contributed to the development of those lines, in particular W.H. Hopkins and N. Eggert.

REFERENCES

- [1] R.H. Dicke, *Astrophys. Journ.*, 153, L101, (1968).
- [2] E.E. Fenimore and T.M. Cannon, *Appl. Optics*, V17, No. 3, p. 337 (1978).
- [3] J.W. Flanagan, et al., *Proc. PAC09*, Vancouver, p.3561 (2009).
- [4] K.J. Kim, *AIP Conf. Proc.* 184 (1989).
- [5] J.D. Jackson, "Classical Electrodynamics," (Second Edition), John Wiley & Sons, New York (1975).
- [6] P.R. Bevington, "Data Reduction and Error Analysis for the Physical Sciences", McGraw-Hill, New York (1969).
- [7] D.P. Peterson, et al., *Proc. IPAC10*, Kyoto, p. 1194 (2010).
- [8] J.W. Flanagan, et al., *Proc. IPAC10*, Kyoto, p. 966 (2010).
- [9] T. Okugi, private communication.
- [10] J.W. Flanagan, et al., *Proc. 7th Meeting of Particle Accelerator Society of Japan*, Himeji, p. 618 (2010).